

Solvent influence on the magnetic field effect of polymethylene-linked photogenerated radical ion pairs

Hans-Gerd Busmann, Hubert Staerk, and Albert Weller

Citation: **91**, (1989); doi: 10.1063/1.457624

View online: <http://dx.doi.org/10.1063/1.457624>

View Table of Contents: <http://aip.scitation.org/toc/jcp/91/7>

Published by the [American Institute of Physics](#)

Solvent influence on the magnetic field effect of polymethylene-linked photogenerated radical ion pairs

Hans-Gerd Busmann, Hubert Staerk, and Albert Weller

Max-Planck-Institut für Biophysikalische Chemie, Abteilung Spektroskopie, D-3400 Göttingen, Federal Republic of Germany

(Received 13 December 1988; accepted 24 April 1989)

The solvent viscosity and polarity dependence of the magnetic field effect in polymethylene-linked radical ion pairs, which were generated by photoinduced intramolecular electron transfer in compounds of the type pyrene-(CH₂)_n-*N,N*-dimethylaniline, has been studied. A stochastic Liouville equation is used, in which the dynamics of the polymethylene chain, the spin Hamiltonian as a function of the varying radical distance (exchange interaction), and a distance-dependent back electron transfer rate are incorporated. The results are compared with predictions made on the basis of the (static) subensemble approximation.

I. INTRODUCTION

Photoinduced electron transfer reactions taking place between electron donor (D) and acceptor (A) molecules lead to the intermediate formation of exciplexes $^1(A^-D^+)$, and radical ion pairs ($^2A^- + ^2D^+$). Their relative (free) energies depend strongly on solvent polarity such that, generally, radical ion pairs are favored in polar solvents, exciplexes in nonpolar solvents.¹⁻³ This applies also to photoinduced electron transfer reactions in polymethylene-linked donor-acceptor systems A-(CH₂)_n-D, abbreviated in the following by A(*n*)D. Through its limited flexibility, however, the polymethylene chain governs the kinetics not only of the electron transfer but also of the back electron transfer processes, in contrast to unlinked systems with free diffusion.⁴⁻²⁰

The general reaction scheme for a polymethylene-linked system presented in Fig. 1 is based on the results of fluorescence studies and flash-photolytic investigations carried out in polar solvents with unlinked and linked A,D systems. In a highly polar solvent, after excitation of the acceptor molecule A, electron transfer from 1D to $^1A^*$ generates the radical ion pair (rip) in its overall singlet state, $^1[{}^2A^-(n) {}^2D^+]$, with a rate constant k_{sr} . The formation of the radical ion pair in its overall triplet state, $^3[{}^2A^-(n) {}^2D^+]$, with a rate designated by $k_{st}(B)$, requires spin realignment in the pair. This is brought about by the hyperfine-coupling-induced (hfc-induced) coherent spin motion of the unpaired electron spins and can be modulated by weak magnetic fields of strength *B* by virtue of the Zeeman effect, and by varying the exchange interaction, which is a function of the A,D distance *r* in $^2A^-$ and $^2D^+$ and thus depends on the chain length (*n*) and chain dynamics. The hfc-induced singlet-triplet transitions can only occur between those radical pair singlet and triplet states which are degenerate within the hfc energy ΔE_{hfc} . The magnitude of ΔE_{hfc} depends on the isotropic hfc constants a_{ik} between the nuclear spins I_{ik} and the unpaired electron spins S_i ; for the systems with A = pyrene and D = *N,N*-dimethylaniline one has $\Delta E_{hfc} = 58$ G.^{13,15,20,21} The spin exchange interaction $J(r)$ between the unpaired electron spins of $^2A^-$ and $^2D^+$, splits the singlet and triplet levels of the

radical ion pair by an amount $2J$, and has an important influence on the magnetic field effect and the product yield, as can be shown experimentally and theoretically. For the compounds used in the present study, the assumption of an exchange interaction through space (solvent) was found to describe the experiments satisfactorily. We therefore give it priority over an interaction mediated through bond (superexchange). Nevertheless, one must ask to what extent superexchange may contribute, since an exchange energy of only 5.8×10^{-7} eV = 50 G ≈ 0.005 cm⁻¹ is required to bring about the observed singlet-triplet splitting. Data for superexchange along flexible aliphatic chains have not been reported.

The instantaneous overall spin state of the radical ion pair determines the recombination route: back electron transfer in the singlet radical pair leads to the singlet ground state, $^1A(n)D$; back electron transfer in the triplet radical pair populates the lowest excited triplet state, $^3A^*(n)D$. Furthermore, close association of $^2A^-$ and $^2D^+$ moieties in

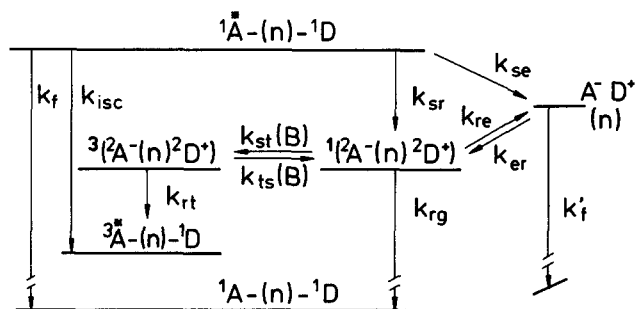


FIG. 1. General reaction scheme for photoinduced intramolecular electron transfer and electron back transfer processes of polymethylene-linked A-(CH₂)_n-D systems in polar solvents; the chain (CH₂)_n is designated by (*n*), the number of chain elements. The left-hand bold superscripts, e.g., in $^3[{}^2A^-(n) {}^2D^+]$ indicate that the radical anion and cation doublets (2) are in an overall triplet (3) spin state. Some rate constants are characterized by pairs of letters which identify the initial and final states of the reaction: singlet state (*s*), triplet state (*t*), radical ion pair (*r*), exciplex state (*e*) and ground state (*g*). The spin multiplicity changes in the radical ion pairs are denoted by the magnetic field-dependent rates $k_{st}(B)$ and $k_{ts}(B)$. Radiative transitions are denoted by k_f and k_f' , and intersystem crossing by k_{isc} .

the singlet radical pair leads (with rate constant k_{re}) to the exciplex state, as has been found recently by studying the magnetic field dependence of exciplex emission in acetonitrile.⁷

As a consequence of the distance dependence of $J(r)$, through which the time evolution of the coupled electron-nuclear spin system is affected, the intramolecular back electron transfer in radical ion pairs of $A(n)D$ is crucially influenced by the stochastic conformational changes of the polymethylene chain. In linked radical pair systems, chain dynamics and spin dynamics are coupled through the exchange interaction more or less permanently throughout the lifetime of the radical pair. The exponential distance dependence of $J(r)$ ^{22,23} alters the influence of the hyperfine and Zeeman interactions in a particularly sensitive way.

The spin-multiplicity changes between the S_0 state of $^1[{}^2A^-(n)D^+]$ and the triplet sublevels T_{-1} , T_0 , and T_{+1} of $^3[{}^2A^-(n)D^+]$, as well as the spin-dependent back electron transfer processes (k_{rg} and k_{ri}), are described by a stochastic Liouville equation. Our approach was strongly influenced by the theoretical treatment (de Kanter *et al.*^{22,23}) of CIDNP experiments with biradicals of cyclic ketones (Closs *et al.*²⁴), and by the so-called static ensemble approximation (SEA) established by Schulten *et al.*¹⁰ The essentials of this treatment have been presented in a qualitative form by Staerk *et al.*⁹ in order to emphasize that the magnetic field-dependent signals of biradicals and polymethylene-linked radical ion pairs are not only related to the conformational distribution but are also strongly dependent on the rate at which the doublet pairs convert between their various conformations. Hence, a considerable loss of information on the equilibrium distribution of the A,D distance is associated with the motional shifting of the exchange spectrum due to the motional broadening/narrowing phenomenon. It was the purpose of the present work to study theoretically and experimentally the spectral motional narrowing and motional shifting aspects of the magnetic field effect in more detail.¹¹

In the experiments the absorbance $A_T(B)$ of the locally excited triplet state ${}^3A^*(n)D$ and the emission intensity $I'(B)$ of the exciplex $^1[A^-(n)D^+]$ were monitored spectroscopically as a function of an external magnetic field B by emission and absorption MODSC spectroscopy.^{7,25,34} This paper deals with the influence (i) of solvents of different viscosity and high polarity, and (ii) of varying polarity and constant viscosity on the reaction kinetics and the magnetic field dependent reaction yields (cf. Table I).

II. EXPERIMENTAL

Compounds $A-(CH_2)_n-D$, 1-(1-pyrene)-*n*-(*p*-*N,N*-dimethylaminophenyl-alkane), [abbreviated as $A(n)D$] with A = pyrene, D = *N,N*-dimethylaniline (DMA) and n = 8,9,10 have been investigated in the solvents acetonitrile (ACN, Merck), in diethylene glycol (DEG, Fluka), in a neutral tenside solution (CEH) and in mixtures of ethyl acetate (ETAC, Merck) with ACN (cf. Table I). CEH is a viscous, highly polar solution of *n*-octyltetraoxyethylene (C_8E_4 , Bachem Feinchemikalien) in water ($pH \approx 9$). The

TABLE I. Solvent parameters, measured at 20 °C.

Solvent ^a	ϵ	η/cP
DEG	32	38
ACN	37.0	0.36
ETAC/ACN		
$x_1 = 0$	37.0	0.36
$x_2 = 31.2$	22.6	0.40
$x_3 = 62.4$	13.4	0.43
$x_4 = 90.4$	7.6	0.44
$x_5 = 100$	6.1	0.44

^a DEG, diethylene glycol [$HO(CH_2)_2O(CH_2)_2OH$]; ACN, acetonitrile (CH_3CN); ETAC, ethyl acetate ($CH_3COOC_2H_5$). ϵ , dielectric constant; η , viscosity, measured with a capillary viscosimeter at 20 °C; x , mol % ETAC.

thermodynamic properties of this system have been described elsewhere.²⁶ The solution used in our studies had a C_8E_4 concentration of 0.18 mol/l and forms a micellar system at room temperature, which ensures sufficient solubility for the compounds to be investigated. The micelle concentration is about one order of magnitude higher than that of the dissolved $A(n)D$ molecules ($\approx 10^{-4}$ mol/l).

Fluorescence lifetimes were measured with a single photon counting apparatus or with a set-up comprising an N_2 laser, a monochromator, a fast photomultiplier and a transient digitizer (R7912, Tektronix). A high pressure xenon lamp was included in this instrument for measurements of the transient radical absorption at 495 nm (pyrene anion absorption). The methods for measuring magnetic field-dependent emission and absorption signals (particularly the triplet absorption of pyrene at 415 nm) have been described earlier.^{7,25} The optical methods which measure the magnetic field effect on yields and rates of spin conversion reactions have been given the collective name "magneto-optically detected spin conversion" spectroscopy (MODSC spectroscopy),^{7,9} to differentiate from microwave techniques (e.g., CIDNP spectroscopy).

The calculation of the triplet yield $\phi_T(B)$ generated from the radical ion pairs has been carried out with the help of lifetime data of the primary excited species and the triplet absorbance $A_T(B)$ of the compound $A(n)D$ and methylpyrene as the reference compound with $k_{sr} = k_{se} = 0$ and $\phi_T(MePy) = 1 - \phi_f = 0.23$ in ACN.²⁷

Rate constants k_{sr} for the compounds $A(n)D$ with n = 7 to 16 have been determined from fluorescence lifetimes to range from 760×10^6 to 470×10^6 s⁻¹ in ACN²⁸ from 59×10^6 to 32×10^6 s⁻¹ in CEH and from 7.4×10^6 to 3.1×10^6 s⁻¹ in DEG.¹¹ These data suggest that the effective viscosity of CEH is intermediate between that of ACN and DEG (cf. Table I).

III. THEORETICAL METHODS

In analogy to an earlier treatment of spin and polymethylene chain dynamics in biradical CIDNP²² we describe the temporal evolution of the spin system in our radical ion pairs and the product formation in the course of back electron

transfer, by the following stochastic Liouville equation (1) (cf. Refs. 12, 22, and 32),

$$\frac{\partial \rho(t)}{\partial t} = [\mathbf{L}_D - i\mathbf{H}^x + \mathbf{Q}_r(\mathbf{L}_K + \mathbf{L}_P)]\rho(t), \quad (1)$$

where $\rho(t)$ is the density matrix of the coupled electron–nuclear spin states and of the product states ${}^3\text{A}^*(n){}^1\text{D}$ and ${}^1\text{A}(n){}^1\text{D}$, as a function of the intramolecular distance r of the radical moieties. The stochastic chain dynamics are described by \mathbf{L}_D , the quantum mechanical spin dynamics by \mathbf{H}^x , and the back electron transfer by \mathbf{Q}_r (r dependence), \mathbf{L}_K (transitions within the radical ion pair spin states) and \mathbf{L}_P (product formation).

A. The polymethylene chain dynamics

We apply a model similar to the restricted diffusion model of de Kanter *et al.*²² The equilibrium distribution $p_0(r)$ of relative ${}^2\text{A}^-$ and ${}^2\text{D}^+$ distances r is divided into N segments of equal width Δr .¹⁰ Its centers at r_m are associated with the probability given in Eq. (2).

$$p_0^m = \int_{r_m - \frac{\Delta r}{2}}^{r_m + \frac{\Delta r}{2}} dr p_0(r). \quad (2)$$

The motion is now described by diffusional jumps (k_d) between different r_m 's. Only transitions between neighboring segments are included, such that

$$\begin{aligned} (\mathbf{L}_D)_{m,k} &= (k_d)(p_0^m/p_0^k)^{1/2} (\delta_{m,k+1} + \delta_{m,k-1}) \\ (\mathbf{L}_D)_{m,m} &= -[(\mathbf{L}_D)_{m,m-1} + (\mathbf{L}_D)_{m,m+1}], \end{aligned} \quad (3)$$

where $(p_0^m/p_0^k)^{1/2}$ is a factor which takes into account different transition rates if one has different probabilities p_0^m for neighboring r_m 's. For $N \rightarrow \infty$ this definition of \mathbf{L}_D assumes the description of diffusion by a Fokker–Planck operator with a continuous variable r .¹⁰ In our study we have chosen a coarse discretization with $N = 10$ so that (k_d) can be associated with a mean rate of change between conformations with different A,D distances, or, more generally, with different exchange interactions.

The distributions $p_0(r)$ for $\text{A}(n)\text{D}$ in a solvent are not available from experiments; therefore one has to use calculated distributions. We have carried out Monte Carlo calculations³⁰ for ${}^2\text{A}^-(n){}^2\text{D}^+$ molecules, taking into consideration the size and the Coulomb attraction of the paramagnetic end groups, which result in structural distributions; an example is shown in Fig. 2 for ${}^2\text{A}^-(9){}^2\text{D}^+$. On the other hand, such structured distributions do not result from molecular dynamics calculations performed for polymethylene chains.¹⁰ For the following calculations smooth curves of the type $p_0(r) = (r - r_0)^a (r_{\text{max}} - r)^b$ were fitted to the structured functions, keeping r_{max} (fully stretched chain) and the mean value of $p_0(r)$, \bar{r} , unchanged. r_0 was arbitrarily chosen as 0.7 nm. The choice of the r_0 value has little actual influence on the yields obtained by simulating the magnetic field effect, because the exchange interaction is very large in this range of A,D distances. Between r_0 and the sandwich distance r_s , the probability density $p_0(r)$ is assumed to be zero

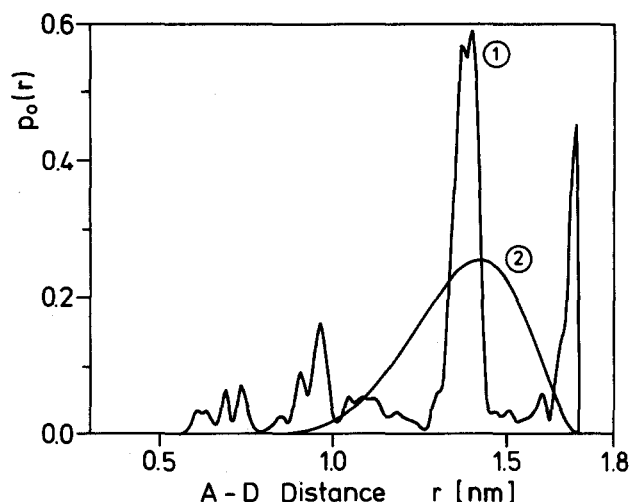


FIG. 2. Calculated probability functions $p_0(r)$ for the A,D distance equilibrium distribution of the radical ion pairs ${}^2\text{A}^-(9){}^2\text{D}^+$. 1 shows the structured distribution obtained with a Monte Carlo method. All calculations in this work are based on the smooth curve 2 of the form $(r - r_0)^a (r_{\text{max}} - r)^b$, obtained by adjustment to the distribution 1 having the parameters $\bar{r} = \sum p_0(r_m)r_m$ and r_{max} in common (see the text). Similarly, smooth curves have been evaluated for $n = 8$ and $n = 10$. The values for r_{max} , a and b are 1.57 nm, 5 and 2 for $n = 8$; 1.70 nm, 5 and 2 for $n = 9$ and 1.83 nm, 5 and 1.5 for $n = 10$, respectively.

for the calculation of triplet yields. This has to be taken as nonzero, if the mechanism of exciplex generation from the radical pair is considered⁷ (see below).

B. The Hamiltonian

The Hamiltonian \mathbf{H} associated with the Liouville operator \mathbf{H}^x contains terms which describe the Zeeman, hyperfine and exchange interactions as in Eq. (4),

$$\begin{aligned} \mathbf{H} &= g\mu_B(\underline{S}_A + \underline{S}_D) + \bar{a}_A \underline{S}_A \underline{I}_A \\ &+ \bar{a}_D \underline{S}_D \underline{I}_D + J(r)(1/2 + \underline{S}_A \underline{S}_D), \end{aligned} \quad (4)$$

where $g\mu_B(\underline{S}_A + \underline{S}_D)$ describes the Zeeman interaction of each electron spin S_i ($i = \text{A,D}$) with an external magnetic field \underline{B} and Δg effects are neglected. In each radical ion the spins \underline{S}_i of the unpaired electrons couple with the nuclear spins \underline{I}_{ik} with a strength which is expressed by the hyperfine coupling (hfc) constants a_{ik} .²⁹ For our calculations the nuclear spin system at each radical is reduced to one spin \underline{I}_i ($I_i = 1/2$). Its hyperfine coupling is given by $\bar{a}_i \underline{S}_i \underline{I}_i$, with the effective hfc constants \bar{a} given by Eq. (5).^{10,18}

$$\bar{a}_i^2 = \frac{4}{3} \sum_k a_{ik}^2 I_{ik} (I_{ik} + 1). \quad (5)$$

Within the scope of the model used to describe the polymethylene chain dynamics, the exchange interaction $J(r)$ between the unpaired electron spins \underline{S}_i is considered to depend only on distance r . We use the exponential r dependence given in Ref. 22, shifted by $r_s = 0.3$ nm to account for the size of the radicals.

$$J(r) = J_0 e^{-\alpha(r-r_s)}, \quad J_0 = 9.46 \times 10^9 \text{ G}, \quad \alpha = 21.36 \text{ nm}^{-1}. \quad (6)$$

C. Back electron transfer

Different approaches are studied in order to be compared with one another and with the experimental results (cf. Sec. IV). In one of our treatments the distance dependence of back electron transfer is modeled by a step function with $\mathbf{Q}_r = \delta_{m,1} \mathbf{I}$, which allows back electron transfer at the encounter distance r_1 only, and in a second treatment a distance independent reaction, $\mathbf{Q}_r = \mathbf{I}$, is assumed. The Liouville matrices for the spin dependence of back electron transfer are given by the following relations:

$$\begin{aligned} \langle IK | \mathbf{L}_K | JL \rangle_m &= -\frac{k_s}{2} (\delta_{KL} \langle I | \mathbf{Q}_S | J \rangle_m + \delta_{IJ} \langle L | \mathbf{Q}_S | K \rangle_m) \\ &\quad - \frac{k_t}{2} (\delta_{KL} \langle I | \mathbf{Q}_T | J \rangle_m + \delta_{IJ} \langle L | \mathbf{Q}_T | K \rangle_m) \quad (7) \end{aligned}$$

$$\langle i | \mathbf{L}_P | j \rangle_m = k_s \langle i | \mathbf{Q}_S^S | j \rangle_m + k_t \langle i | \mathbf{Q}_T^T | j \rangle_m,$$

where I, J, K, L run through all electron-nuclear spin states and i, j through all states of the density matrix pertaining to m . $\mathbf{Q}_S, \mathbf{Q}_T$ project onto the electron spin states, and $\mathbf{Q}_S^S, \mathbf{Q}_T^T$ onto the transition elements from the spin states to the product states. The parameters k_s and k_t are the rates of back electron transfer. In the case of $\mathbf{Q}_r = \delta_{m,1} \mathbf{I}$ they give back electron transfer rates at r_1 only and compete with the diffusional escape from r_1 . The radical pair lifetime τ_{rip} depends on $k_s, k_t, p_0(r)$ and k_d . On the other hand, in the case of $\mathbf{Q}_r = \mathbf{I}$ the k_s, k_t are of the order of magnitude of $1/\tau_{rip}$, which is independent of $p_0(r)$ and k_d (for $k_s \equiv k_t = k$ it follows that $k = 1/\tau_{rip}$).

D. Solution of the stochastic Liouville equation

The observable which is appropriate for a comparison between theory and experiment is the magnetic field dependence of the triplet yield $\phi_T(B)$. After the reactions forming the triplet state ${}^3\text{A}^*(n) {}^1\text{D}$ are terminated, they result in Eq. (8).

$$\begin{aligned} \phi_T(B) &= \lim_{t \rightarrow \infty} \sum_m \rho_{TTm}(t) \\ &= \lim_{s \rightarrow 0} s \sum_m \alpha_{TTm}(s) \quad [\text{cf. Eq. (9)}]. \quad (8) \end{aligned}$$

To calculate $\phi_T(B)$ from Eqs. (1) and (8) a real, linear system of equations is solved, which result from a Laplace-transform \mathcal{L} and from a unitary transformation \mathbf{U} of Eq. (1)

$$\alpha = \mathbf{U} \mathcal{L} \rho; \mathbf{R}^x = \mathbf{U}^\dagger \mathbf{H}^x \mathbf{U} \quad (9)$$

$$[s\mathbf{I} + \mathbf{L}_D + \mathbf{R}^x - \mathbf{Q}_r(\mathbf{L}_K + \mathbf{L}_P)] \alpha = \alpha^0, \quad (10)$$

α^0 contains the population of the spin states at time $t = 0$. The radical ion pair generation at the encounter distance corresponds to a uniform population of all Z nuclear spin states of the S_0 electron spin state $(\alpha^0)_m = (1/Z) \mathbf{Q}_S \delta_{m,1}$. An equilibrium distribution at time $t = 0$ corresponding to $p_0(r)$ is described by $(\alpha^0)_m = (1/Z) \mathbf{Q}_S \rho_0^m$.

For comparison with experimental results, the calculation of the triplet yield $\phi_T(B)$ is carried out with both a radical ion pair generation and a back electron transfer oc-

curing at the encounter distance only. In order to determine sets of values for k_s, k_t and k_d which give appropriate radical ion pair lifetimes a numerical integration of Eq. (1), truncated to include only the diffusional and back electron transfer processes, was carried out with $k_s = k_t$.

E. The subensemble approximation (SEA)³¹

In a further simplified treatment introduced by Schulten and Bittl,¹⁰ the stochastic ensemble with the distance and hence time dependent Hamiltonian characterized by $J = J[r(t)]$, is approximated by isolated subensembles with constant exchange interaction and thus time independent Hamiltonian. In this approximation the triplet yields of the subensembles, $\phi_T(B, 2J)$,¹⁰ are weighted by the spectral distribution function $w(2J)$ of the exchange interaction and finally added, according to

$$\phi_T(B) = \int_{-\infty}^{\infty} d2J w(2J) \phi_T(B, 2J). \quad (11)$$

The exchange spectrum

$$w(2J) = \frac{2}{\pi} \text{Re} \sum_{m, m'} \langle m' | [i(2J - 2J\mathbf{I}) - \mathbf{L}_D]^{-1} | m \rangle p_0^m \quad (12)$$

is a dynamic distribution function of exchange interactions, developed from the Kubo theory for stochastically modulated classical oscillators,³² where m, m' designate the subensembles and $\mathbf{J}_{m, m'} = 2J(r_m) \delta_{m, m'}$. In essence, $w(2J)$ incorporates the influence of the rate of conformational changes on the overall (final) triplet yield. In the basic SEA model, radical ion pair formation and back electron transfer are considered to be independent of the A, D distance; furthermore $k_s \equiv k_t = 1/\tau_{rip}$ is assumed.

Under the same restrictions and with $k = 1/\tau_{ion}$, Eq. (1) can be modified to

$$\frac{\partial \rho(t)}{\partial t} = [\mathbf{L}_D - i\mathbf{H}^x - k\mathbf{I}] \rho(t). \quad (13)$$

This equation has been solved recently by Bittl *et al.*¹²

Figure 3 shows $w(2J)$ spectra for a specific $p_0(r)$ distribution (cf. Fig. 2, distribution 2) but varying mobility, expressed by k_d ; only distance variations are considered. For large k_d the spectra undergo "motional narrowing." The exponential dependence of the exchange interaction on distance implies an asymmetrical "motional deformation" and "motional shifting" of the $w(2J)$ spectra with changing k_d . The maxima shift to higher $2J$ values with increasing k_d ; broadened distributions at intermediate values of k_d narrow again as $k_d \rightarrow \infty$. It is this behavior of the dynamic $w(2J)$ spectra, indicating a solvent viscosity dependence of the $\phi_T(B)$ distributions, which motivated us to perform experiments with varying solvent parameters^{9,11,34} and to carry out simulations of the experimental results.

IV. RESULTS AND DISCUSSION

First we discuss triplet yields for A(9)D in high polarity solvents of different viscosities. Figure 4(a) shows the ex-

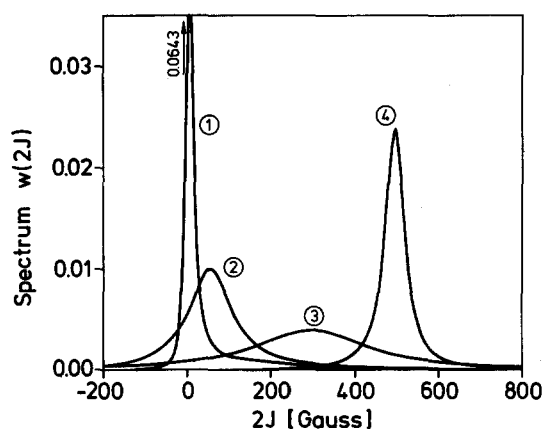


FIG. 3. Spectra of the exchange interaction as defined by Eq. (12). The probability distribution $w(2J)$ is plotted vs the singlet-triplet splitting $2J$ for varying chain dynamics (k_d) but otherwise identical conditions. The values for k_d are 1×10^9 , 50×10^9 , 1×10^{12} , and $20 \times 10^{12} \text{ s}^{-1}$ for the curves 1, 2, 3, and 4, respectively.

perimentally determined magnetic field-dependent triplet yields $\phi_T(B/G)$ in the solvents DEG, CEH and ACN, i.e., solvents with decreasing viscosity. The absolute triplet yields are much higher in ACN than in CEH and DEG.

To compare these experimental results with theoretical curves, the stochastic Liouville equation was solved under the conditions for which radical ion pair formation and back electron transfer occur only at the encounter distance. The results of these calculations are shown in Fig. 4(b). The

simulation of the behavior of the ensemble upon variation of the solvent viscosity is achieved by variation of k_d but keeping the other parameters constant; Eqs. (1)–(10) have been used. At $B = 0$ one sees an initial increase ($4 \rightarrow 3$) of the triplet yield with decreasing k_d , and after going through a maximum, the yield decreases ($3 \rightarrow 2 \rightarrow 1$). B_{\max} and the relative height of the triplet yield maximum, $R_{\max} = 1 - \phi_T(B)/\phi_T(0)$ at B_{\max} , decrease with decreasing k_d . Comparing Fig. 4(a) with Fig. 4(b) one can immediately see that variation of k_d in the calculation can simulate the trend, both of the shift of the maxima and of the absolute yields, rather well. Curve 3 in Fig. 4(b) corresponds to $k_d = 1 \times 10^{12} \text{ s}^{-1}$. With this rate constant the calculated radical pair lifetime becomes equal to the experimental value at zero magnetic field, $\tau_{\text{rip}} = 14.7 \text{ ns}$ in ACN.

Figure 4(d) shows the results of a simulation using the basic SEA model at different solvent viscosities represented by varying k_d . Similar to Fig. 4(b), B_{\max} decreases with decreasing k_d , but unlike the results in Figs. 4(b) and 4(a), the triplet yield at zero magnetic field $\phi_T(0)$ increases monotonically with decreasing k_d . This behavior can be understood if one remembers that in the basic SEA model both radical ion pair generation and back electron transfer are assumed to be independent of the chain conformation. Clearly, the inclusion of a distance dependence of the back electron transfer, which also makes allowance for the diffusion processes necessary for electron spin-multiplicity changes, leads to the observed decrease of $\phi_T(0)$. This influence can also be seen by comparing Figs. 4(b) and 4(c). The

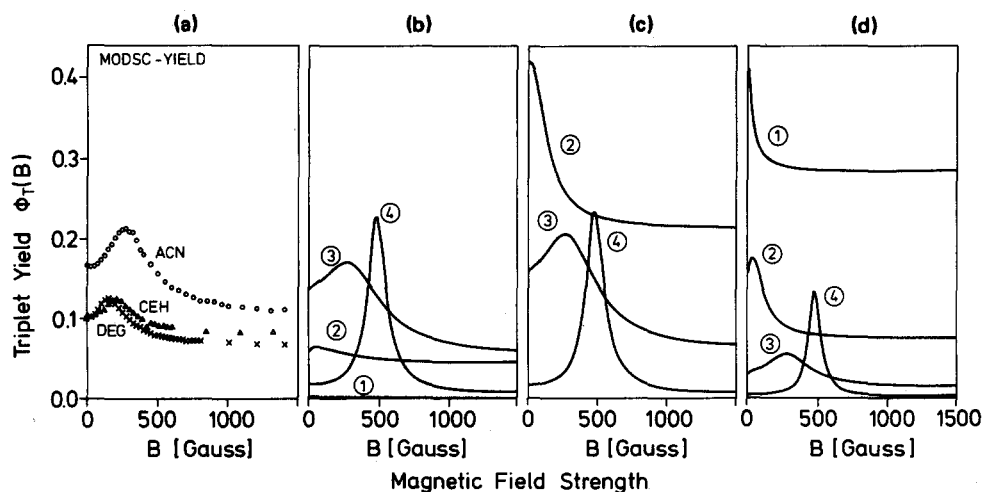


FIG. 4. Magnetic field effect of ${}^2\text{A}^-({}^9)\text{D}^+$ in solvents of strongly varying viscosity and high polarity as a function of the applied magnetic field strength in the range from $B = 0$ to 1500 G. Comparison of experimental results (a) with different theoretical models (b) and (c). (a) Triplet yields $\phi_T(B)$ from MODSC experiments carried out in acetonitrile (ACN, \circ), in a neutral tenside solution (CEH, Δ) and in diethylene glycol (DEG, \times); yields are corrected for the triplets which are not generated by the radical pair mechanism (cf. Fig. 1). (b) Triplet yields $\phi_T(B)$ calculated with the stochastic Liouville equation for varying chain dynamics (different diffusional rate constants k_d). In order to simulate the experimental system, the generation of the radical ion pair and the back electron transfer (BET) are assumed to take place at the encounter distance $r_1 = 7.5 \text{ nm}$ only. The values for k_d are 1×10^9 , 50×10^9 , 1×10^{12} , and $20 \times 10^{12} \text{ s}^{-1}$ for the curves 1, 2, 3, and 4, respectively. The values of the rate constants which describe the deactivation of the radical ion pair, are $k_s = k_r = 3 \times 10^{12} \text{ s}^{-1}$. In curve 3, the lifetime of the radical ion pair is the same as the experimental value in acetonitrile (ACN) at $B = 0 \text{ G}$, $\tau_{\text{rip}} = 14.7 \text{ ns}$. (c) Triplet yields $\phi_T(B)$ calculated with the stochastic Liouville equation for varying chain dynamics (different k_d 's) in order to compare the approach given in (b) with the (static) subensemble approximation (SEA) treatment given in (d). The generation of the radical ion pair is assumed to take place at the encounter distance only, whereas the back electron transfer (BET) is assumed to be independent of r ; $k_r^{-1} = k_s^{-1} = 14.7 \text{ ns}$ [cf. (b)]. The values for k_d are the same as in (b). (d) Triplet yields $\phi_T(B)$ calculated with the (static) subensemble approximation for varying chain dynamics (different k_d 's). Both, the generation of the radical ion pair and the back electron transfer are independent of r . The lifetime of the radical ion pair is taken to be the experimental value at $B = 0 \text{ G}$, $\tau_{\text{rip}} = 14.7 \text{ ns}$. The values of k_d are the same as in (b); the corresponding dynamic $2J$ distributions are shown in Fig. 3.

curves in Fig. 4(c) have been obtained with the stochastic Liouville equation as in Fig. 4(b), but with the back electron transfer being independent of r .

In a particular solvent the magnetic field values of the maxima in the triplet yield, B_{\max} , have been found to decrease with increasing chain length n .^{5-9,11} Figure 5(a) gives the measured relative triplet yields $\phi_T(B)/\phi_T(0)$ of compounds A(n)D with different chain length $n = 8, 9, 10$ in the solvent ACN. B_{\max} and the width of the maxima decrease with increasing chain length n . Figure 5(b) shows calculated curves which have been fitted to the experimental curves with the following assumptions: (i) electron transfer is permitted at the encounter distance only, (ii) the values for the kinetic parameters k_d , k_s and k_t are assumed to be solvent independent for different numbers n of CH₂ groups, (iii) the $\rho_0(r)$ distributions for the fits in the solvent ACN are smoothed curves derived from the Monte Carlo distributions (cf. Fig. 2, curve 2). It has been shown above that, in principle, the decrease of the absolute triplet yield and the decrease of B_{\max} with increasing solvent viscosity can be well understood. For the solvent DEG, however, it turns out that the simulation of B_{\max} , together with the height of the maxima, by varying just k_d alone does not yield a good fit. In the calculations, anisotropic terms in the spin Hamiltonian which may result from torsional motion about the bonds connecting the radical ion moieties to the chain, have not been considered explicitly. Neither the relative angular dependence of the exchange interaction nor its time dependence are known for such clearly important motions. Furthermore in the more viscous solvents the equilibrium distribution may not be attained prior to the back electron transfer reaction. A consideration of these effects within the theoretical framework discussed so far requires a more de-

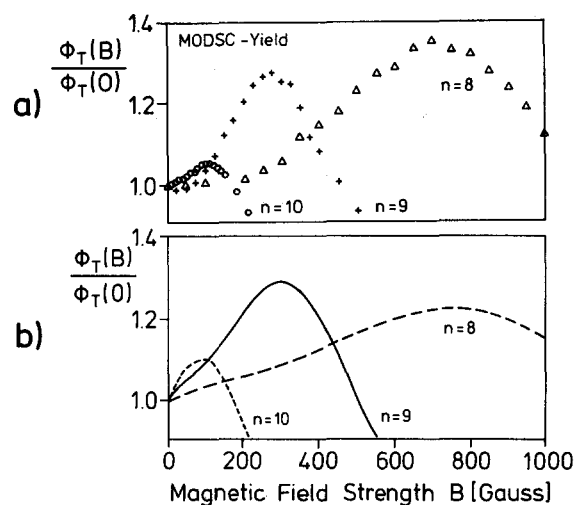


FIG. 5. Chain length dependence of the relative triplet yield $\phi_T(B)/\phi_T(0)$ as a function of the magnetic field strength in the range from $B = 0$ to 800 G in the solvent acetonitrile (ACN). (a) MODSC yields for $n = 8$ (Δ), $n = 9$ ($+$) and $n = 10$ (\circ); (b) simulated magnetic field dependence for $n = 8$ (---), $n = 9$ (—) and $n = 10$ (---). The following parameters were used for the simulation: $k_d = 1.2 \times 10^{12} \text{ s}^{-1}$, $k_s = 2 \times 10^{12} \text{ s}^{-1}$, $k_t = 1.5k_s$. For the $\rho_0(r)$ distributions smooth curves of the form $(r-r_0)^n \cdot (r_{\max} - r)^b$ have been used (cf. Fig. 2). The absolute error of the difference between the measured and calculated absolute triplet yields is less than 0.02.

tailed description of chain dynamics.

Further experiments which demonstrate the motional shifting and motional narrowing concept are the following. Solvent mixtures with roughly the same macroscopic viscosity but varying bulk dielectric properties (cf. Table I) are assumed to preserve the same molecular dynamics, but to differ in other parameters which have an influence on the electron transfer and back electron transfer rates. As a first example, Fig. 6(a) gives the magnetic field dependence of the relative exciplex yield $I'(B)/I'(0)$; the numbers 1–4 in Figs. 6(a) and 6(b) designate the mole ratios of ETAC, x_1, \dots, x_4 . Figure 6(b) shows the corresponding relative triplet absorbance signals $A_T(B)/A_T(0)$. The minima (B_{\min}) in the exciplex curves and the maxima (B_{\max}) in the absorption curves occur at the same field strength and are most pronounced for the solvent acetonitrile (curve 1). Earlier studies of the magnetic field sensitivity of the exciplex emis-

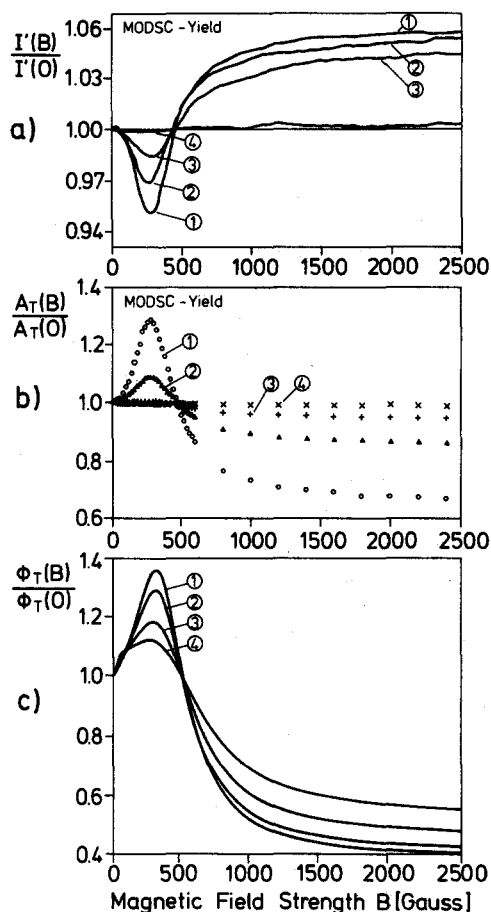
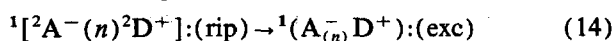


FIG. 6. (a) and (b) Magnetic field effect of ${}^2\text{A}^-(9){}^2\text{D}^+$ in solvent mixtures of constant viscosity and different polarity as a function of the applied magnetic field strength in the range from $B = 0$ to 2500 G. (a) The relative exciplex emission $I'(B)/I'(0)$ and (b) the relative triplet absorbance $A_T(B)/A_T(0)$ are shown in mixtures of ethyl acetate (ETAC) with acetonitrile (ACN). The mole ratios x_i of ETAC are 0, 31, 62, and 94 for the curves 1, 2, 3 and 4, respectively. (c) Relative triplet yields $\phi_T(B)/\phi_T(0)$ calculated with the stochastic Liouville equation for varying rates of radical ion pair deactivation; the values for k_d are 3.0×10^{12} , 2.0×10^{12} , 1.0×10^{12} , and $0.5 \times 10^{12} \text{ s}^{-1}$ for the curves 1, 2, 3, and 4, respectively, and $k_s = 1.5k_d$. The generation of the radical ion pair and the back electron transfer are assumed to take place at the encounter distance only. The rate of chain interconversion, $k_d = 1.2 \times 10^{12} \text{ s}^{-1}$, and the $\rho_0(r)$ distribution (curve 2 in Fig. 2) have been kept constant.

sion have provided unequivocal evidence for an intramolecular exciplex formation directly from the radical ion pair species,⁷ according to the scheme



for highly polar solvents such as ACN (cf. Fig. 1). The corresponding curves (1) in Fig. 6(a) and 6(b) confirm these earlier results both with respect to the values of $B_{\text{min}}/B_{\text{max}} \approx 280$ G and the relative yields. Equation (14) represents the second (exothermic or endothermic) part of a photoinduced two-step reaction for which we earlier suggested the term "harpooning."^{4,5,7,33}

In the solvent mixtures with increasing mole fraction of ETAC, i.e., decreasing bulk dielectric constant, the magnetic field effect gradually disappears. A magnetic field effect is not observed in ETAC alone ($x = 100$, $\epsilon = 6.1$).

In the context of the motional shifting hypothesis the most interesting result of these experiments is the fact that for all solvent mixtures B_{min} and B_{max} have practically the same value (280 G). The collapse of the extrema in the experimental curves is another important feature, and a more extended discussion will be given elsewhere. It is essentially due to the partitioning of the exciplex and triplet formation routes with decreasing solvent polarity. Magnetic field-independent exciplex formation can occur directly from the locally excited singlet state with rate constant k_{se} (cf. Fig. 1). Similarly, the magnetic field-independent intersystem crossing from the locally excited singlet state and from the exciplex contributes to the overall triplet yield. The result is a reduction of the magnetic field effect. However, particularly in the high polarity range [curves 1 and 2 in Figs. 6(a) and 6(b)], additional explanations for the relative signal collapse are needed, namely an influence of solvent dielectric properties on the back electron transfer rate. For example, the lifetimes of the pyrene radical have been measured to be $\tau_{\text{rip}}(x_1) = 14.7$ ns and $\tau_{\text{rip}}(x_2) = 29.7$ ns at $B = 0$ G. This is a very interesting result, since thermodynamic calculations with well-established expressions for the free enthalpy change of the radical pair and the exciplex,² predict only a small change in free enthalpy $\Delta G_{\text{rip}}^\epsilon$ and $\Delta G_{\text{exc}}^\epsilon$, when the bulk dielectric constant is varied from 37.5 (x_1) to 22.6 (x_2).

Within the framework of the stochastic Liouville equation, different radical ion lifetimes at equal rates for conformational changes k_d can be obtained by varying k_s and k_t . Figure 6(c) shows calculated triplet yields $\phi_T(B)/\phi_T(0)$ for varying rate constant k_s ($k_s/k_t = \text{const}$) for the back electron transfer, but with otherwise identical assumptions. The features common to all three sets of curves of Figs. 6(a)–6(c) are that they cross the relative value of $\phi_T(B)/\phi_T(0) = 1$ or $I'(B)/I'(0) = 1$, respectively, at about the same point, and the extrema appear in all three cases at about the same magnetic field strength. In Fig. 6(c), the low relative triplet yield at high magnetic field strengths is probably the result of the strongly reduced nuclear spin system assumed for the calculations.

V. SUMMARY

In the theoretical part of this paper we have outlined briefly the methods currently available to describe the gen-

eral radical pair mechanism, i.e., the nuclear hyperfine interaction, modulated by the stochastic folding and torsional motion of the linking molecular chain, which is predicted to lead to a motional deformation in the magnetic field dependence of the reaction yield.

Experimentally, the magnetic field dependent triplet yield of the systems investigated exhibits a maximum at the magnetic field strength B_{max} . This is the field strength corresponding approximately to the most frequently occurring exchange interaction in the radical ion pair. The position of the minimum B_{min} in the magnetic field dependence of the exciplex yield is found to coincide with that of B_{max} . According to theoretical considerations, the spatial distribution (in a simple model, the A,D distance) of the polymethylene-linked radical ions is not the only important parameter determining the characteristic magnetic field strength; B_{max} ($= B_{\text{min}}$) also depends strongly on the rate at which the doublet pairs convert among their various conformations. The experiments show that, with varying solvent viscosity, this rate and thus B_{max} ($= B_{\text{min}}$) can change significantly. On the other hand, a decrease in the solvent polarity does not seem to alter the spin dynamics, but influences the thermodynamics of the A–D system and partitions, e.g., the primary fluorescence quenching reaction in other directions (exciplex formation) and possibly affects also the back electron transfer processes.

The application of an extended stochastic Liouville equation, that takes into account a distance-dependent back electron transfer, was found to be essential to account quantitatively for several important details, e.g., the absolute triplet yields at zero magnetic field, including the decrease of B_{max} (B_{min}) with increasing solvent viscosity.

ACKNOWLEDGMENTS

We would like to thank Dr. W. Kühnle and his co-workers for preparing and purifying the model compounds. We thank B. Frederichs and H. Meyer for technical assistance. Dr. R. Strey suggested the neutral amphiphiles as a solvent and gave instructions on its preparation. Dr. R. Bittl and Professor K. Schulten made available to us a copy of the diploma work of R. Bittl (TU München, 1985) which was very helpful. We acknowledge discussions with Dr. J. Ihlemann and Dr. R. Treichel. This work has been supported by the Deutsche Forschungsgemeinschaft through Sonderforschungsbereich SFB 93 "Photochemistry with Lasers."

¹H. Leonhardt and A. Weller, *Z. Phys. Chem.* **29**, 277 (1961); *Ber. Bunsenges. Phys. Chem.* **67**, 791 (1963); A. Weller, *Nobel Symposium Series Vol. V*, edited by S. Claesson, (Almqvist & Wiksell, Stockholm, 1967), p. 413.

²A. Weller, *Z. Phys. Chem.*, **133**, 93, (1982), and references therein.

³H. Schomburg, H. Staerk, and A. Weller, *Chem. Phys. Lett.* **21**, 433 (1973); **22**, 1 (1973).

⁴H. Staerk, R. Mitzkus, W. Kühnle, and A. Weller, in *Ultrafast Phenomena III*, edited by K. B. Eisenthal, R. Hochstrasser, and W. Kaiser, Springer Series of Chemical Physics (Springer, Berlin, 1982), Vol. 23, p. 205.

⁵H. Staerk, W. Kühnle, R. Mitzkus, R. Treichel, and A. Weller, in *Ultrafast Phenomena IV*, edited by D. H. Auston and K. B. Eisenthal, Springer

- Series of Chemical Physics, (Springer, Berlin, 1984), Vol. 38, p. 380.
- ⁶A. Weller, H. Staerk, and R. Treichel, *Faraday Discuss. Chem. Soc.* **78**, 271 and 332 (1984).
- ⁷H. Staerk, W. Kühnle, R. Treichel, and A. Weller, *Chem. Phys. Lett.* **118**, 19 (1985).
- ⁸R. Treichel, Dissertation, University of Göttingen, 1985.
- ⁹H. Staerk, R. Treichel, and A. Weller, in *Biophysical Effects of Steady Magnetic Fields*, edited by G. Maret, J. Kiepenheuer, and N. Bocarra, Springer Proceedings in Physics (Springer, Berlin, 1986), Vol. 11, p. 85.
- ¹⁰K. Schulten and R. Bittl, *J. Chem. Phys.* **84**, 9 (1986); R. Bittl, Diplomarbeit, Techn. Univ. München, (1985); R. Bittl and K. Schulten, in *Biophysical Effects of Steady Magnetic Fields*, edited by G. Maret, J. Kiepenheuer, and N. Bocarra, Springer Proceedings in Phys. (Springer, Berlin, 1986), Vol. 11, p. 90.
- ¹¹H.-G. Busmann, Dissertation, University of Göttingen, 1987.
- ¹²R. Bittl and K. Schulten, *Chem. Phys. Lett.* **146**, 58 (1988).
- ¹³K. Schulten, H. Staerk, A. Weller, H.-J. Werner, and B. Nickel, *Z. Phys. Chem.* **101**, 371 (1976).
- ¹⁴M. E. Michel-Beyerle, R. Haberkorn, W. Bube, E. Steffens, H. Schröder, H. J. Neusser, and E. Schlag, *Chem. Phys.* **17**, 139 (1976).
- ¹⁵H.-J. Werner, H. Staerk, and A. Weller, *J. Chem. Phys.* **68**, 2419 (1978).
- ¹⁶H. Schomburg, H. Staerk, A. Weller, and H.-J. Werner, *Chem. Phys. Lett.* **56**, 399 (1978).
- ¹⁷Z. Schulten and K. Schulten, *J. Chem. Phys.* **66**, 4616 (1977).
- ¹⁸K. Schulten and P. G. Wolynes, *J. Chem. Phys.* **68**, 3292 (1978).
- ¹⁹F. Nolting, H. Staerk, and A. Weller, *Chem. Phys. Lett.* **88**, 523 (1982).
- ²⁰A. Weller, F. Nolting, and H. Staerk, *Chem. Phys. Lett.* **96**, 25 (1983).
- ²¹H. Staerk, R. Treichel, and A. Weller, *Chem. Phys. Lett.* **96**, 28 (1983).
- ²²F. J. J. de Kanter, J. H. den Hollander, A. H. Huizer, and R. Kaptein, *Mol. Phys.* **34**, 875 (1977).
- ²³F. J. J. de Kanter, R. Z. Sagdeev, and R. Kaptein, *Chem. Phys. Lett.* **58**, 334 (1978).
- ²⁴G. L. Closs and C. E. Doubleday, *J. Am. Chem. Soc.* **95**, 2736 (1973).
- ²⁵R. Treichel, H. Staerk, and A. Weller, *Appl. Phys. B* **31**, 15 (1983).
- ²⁶M. Kahlweit and R. Strey, *Angew.* **97**, 655 (1985); V. Degiorgio, in *Proceedings of the International School of Physics Enrico Fermi—Physics of Amphiphiles: Micelles, Vesicles and Microemulsions* (North-Holland, Amsterdam, 1985).
- ²⁷K. A. Zachariasse (private communication).
- ²⁸A. Weller, in *Supramolecular Photochemistry*, edited by V. Balzani, NATO ASI Ser. C (Reidel, Dordrecht, 1987), Vol. 214, p. 343.
- ²⁹K. M. Salikhov, Yu. N. Molin, R. Z. Sagdeev, and A. L. Buchachenko, in *Spin Polarization and Magnetic Effects in Radical Reactions*, edited by Yu. N. Molin (Elsevier, Amsterdam 1984), Vol. 22.
- ³⁰M. Lal and D. Spencer, *Mol. Phys.* **22**, 649 (1971).
- ³¹The authors of Ref. 10 call this approach the static ensemble approximation. We feel the term "static" could be misleading. Since the separate treatment of the chain dynamics comprises the full ensemble, whereas the spin dynamics is treated only for static subensembles, we prefer to give SEA the name "subensemble approximation."
- ³²R. Kubo, in *Fluctuation, Relaxation and Resonance in Magnetic Systems*, edited by D. ter Haar (Oliver and Boyd, Edinburgh, (1962), p. 23; *J. Math. Phys.* **4**, 174 (1963); in *Stochastic Processes in Chemical Physics* edited by K. E. Shuler (Interscience, New York, 1969); *Adv. Chem. Phys.* **15**, 101 (1969).
- ³³M. Schulz, Dissertation, University of Göttingen, 1974.
- ³⁴H. Staerk, H.-G. Busmann, W. Kühnle, and A. Weller, *Chem. Phys. Lett.* **155**, 603 (1989).